Role of pointlike topological excitations at criticality: From vortices to global monopoles

Nuno D. Antunes,[1] Luís M. A. Bettencourt,[2] and Martin Kunz[3]
[1]*Centre for Theoretical Physics, University of Sussex, Falmer, Brighton BN1 9QJ, United Kingdom*
[2]*Center for Theoretical Physics, Massachusetts Institute of Technology, Building 6-308, Cambridge, Massachusetts 02139*
[3]*Department of Astrophysics, Oxford University, Keble Road, Oxford OX1 3RH, United Kingdom*
(Received 17 January 2002; revised manuscript received 5 April 2002; published 21 June 2002)

We determine the detailed thermodynamic behavior of vortices in the O(2) scalar model in two dimensions (2D) and of global monopoles in the O(3) model in 3D. We construct numerical techniques, based on cluster decomposition algorithms, to analyze the point defect configurations. We find that these criteria produce results for the Kosterlitz-Thouless temperature in agreement with a topological transition between a polarizable insulator and a conductor, at which free topological charges appear in the system. For global monopoles we find no pair unbinding transition. Instead a transition to a dense state where pairs are no longer distinguishable occurs at $T<T_c$, without leading to long-range disorder. We produce both extensive numerical evidence of this behavior as well as a semianalytic treatment of the partition function for defects. General expectations for $N=D>3$ are drawn, based on the observed behavior.

DOI: 10.1103/PhysRevE.65.066117 PACS number(s): 64.60.Fr, 11.27.+d, 75.10.Hk, 98.80.Cq

I. INTRODUCTION

The detailed understanding of the many roles played by nonperturbative topological excitations in the dynamics and thermodynamics of statistical models and field theories is one of the most fascinating and largely unresolved issues of many-body systems.

In the simplest Abelian gauge field theories vortices are intimately connected with the existence of a superconducting state in type-II materials [1]. Excitations carrying topological numbers (instantons, monopoles, vortices) are also thought to be the best candidates for an explanation of confinement in non-Abelian gauge theories [2]. In the context of statistical models with global symmetries it has long been understood that topological excitations can lead to the onset of phase disorder at high temperatures [3]. Their presence in configurations in one spatial dimension (1D) in models with local interactions down to $T=0^+$ prohibits, in fact, the establishment of long-range order at any finite temperature [4,5]. In dissipative dynamical systems the long-range disorder and temporal scaling present in the long-time limit of phase ordering kinetics can also be understood in terms of topological excitations [6,7].

Several canonical examples illustrate the role of topological excitations in bringing about phase transitions [3,8,9]. Among them the best known is the Kosterlitz-Thouless (KT) transition. At low temperatures the O(2) model in 2D exhibits algebraic long-range order, which would persist to all temperatures in the absence of topological excitations. The advent of disorder at high temperatures is due to vortex excitations, which appear as free charges at the Kosterlitz-Thouless temperature T_{KT}.

Recently, due largely to increases in computational power and improved methods, many of these systems have become available to direct quantitative study. This is particularly true of models with global symmetries, embodied to a large extent by O(N)-symmetric magnets or field theories.

An interesting question then is what happens as we progressively stray away from cases where topological excitations are known to dominate critical thermodynamic behavior? In this article we investigate this question for point defects in O(N) models in D dimensions, taking as a starting point the Kosterlitz-Thouless transition, i.e., the case $D=N=2$. The successes of the renormalization group at characterizing critical behavior in $D>2$ suggest that physics in the critical region is dominated by perturbative excitations (spin waves). In particular as N increases, mean-field descriptions become suitable. In this limit thermodynamic effects due to topological defects are totally unexpected. What then becomes of the topological excitations? Do they disappear from the spectrum as likely fluctuations, or do they still occur but in a manner that does not lead to long-range disorder?

The answers to these questions are necessary underpinnings for a general picture of the behavior of topological excitations both in equilibrium and as seeds for the formation of topological defects upon cooling. Current understanding of the formation and evolution of topological defects [10,11] in cosmology and in condensed matter requires the presence in the disordered phase of fluctuations, which upon cooling can result in long-lived topological *defects*. Familiar examples are long vortex strings (cosmic strings) or well-separated monopole-antimonopole pairs. If these configurations are rare in thermal equilibrium, above the transition, their abundances will be very small and short lived upon cooling. Such behavior may have significant phenomenological implications and shed new light on old questions such as the monopole problem in cosmology [12] or the planning of defect formation experiments in condensed matter systems.

In this paper we study in detail the similarities and differences between the statistical behavior of vortices in the O(2) 2D model and of global monopoles in the 3D O(3) model, in thermal equilibrium. For reasons that we make clear in Sec. II this step, between $N=D=2$ and $N=D=3$, straddles the boundary between a case where topological excitations drive an order-disorder transition (the former) and a case where topological excitations may be expected to become thermodynamically irrelevant, at least for the long-distance physics

that is characteristic of criticality.

This problem has been investigated in several instances in the past, leading to important insights, but a consistent picture of the thermodynamics of global monopoles has yet to emerge. The strongest evidence for an important role played by monopoles at criticality in the O(3) model in 3D comes from the study of modified partition functions, which include monopole suppression terms [13,14]. Lau and Dasgupta [13] showed that the introduction of one such term, suppressing *all* monopole fluctuations, results in the disappearance of critical behavior altogether. Later Kamal and Murthy [14] used a different monopole suppression term, which allowed monopole-antimonopole pairs with lattice space separation only. They found a new second-order transition, with exponents different from those of the conventional O(3) universality class. Lau and Dasgupta [13] also claimed that at the critical temperature of the conventional O(3) model the temperature derivative of the monopole density $d\rho/dT$ exhibits a divergence, which they argued would signal monopole-antimonopole pair unbinding. This claim was also taken up by Huang, Kolke, and Polonyi [15], who conjectured that the phase transition in the O(3) model would then be driven by monopole-antimonopole separation, in analogy with the vortex unbinding that triggers the Kosterlitz-Thouless transition in the O(2) model in 2D. Later the evidence for a diverging $d\rho/dT$ disappeared with a high precision cluster algorithm study by Holme and Janke [16], who showed that $d\rho/dT$ behaves like the specific heat, which does not diverge at T_c. Moreover, Bitar and Manousakis [17] searched for unbound monopoles by considering phase correlations along closed loops in space. They concluded that no such configurations could be found, implying that the unbinding of monopoles plays no role in the critical thermodynamics of the O(3) model in $D=3$.

This body of evidence paints a complex picture of the behavior of monopoles at criticality in the O(3) magnet in 3D. It suggests that while monopole degrees of freedom are important in bringing about disorder with increasing temperature and contribute nontrivially to the physics of the $N=3$, $D=3$ universality class, they are not essential for the establishment of long-range disorder. In particular their behavior may not be critical at all at T_c. Thus, drawing analogies with the Kosterlitz-Thouless transition may provide a poor guide to their thermodynamics.

The present paper is dedicated to elucidating some of these questions through a detailed comparative study of the critical behavior of monopoles and vortices in the O(3) Heisenberg magnet and the $N=D=2$ XY model, respectively. This article is organized as follows. In Sec. II we review and extend standard free energetic arguments for point defects of O(N) scalar models in D dimensions. These arguments are both simple and very powerful in determining whether topological transitions can occur and in elucidating their nature. In Sec. III we characterize the thermodynamic behavior of vortices in the Kosterlitz-Thouless transition by analyzing their statistical clustering properties. We find, in agreement with the Kosterlitz-Thouless paradigm, that the transition proceeds by pair unbinding, which can be observed prior to a vortex percolation transition. The latter occurs at a slightly higher temperature, approximately where the specific heat peaks. Armed with this quantitative information of the KT transition and the analytical arguments of Sec. II, we analyze, in Sec. IV, the statistical properties of monopoles in the O(3) model in 3D. We find no unbinding transition as expected on energetic grounds alone, but still a percolation transition occurs at a temperature below T_c. We develop methods to describe the monopole behavior quantitatively and argue that the observed percolation transition can occur without leading to long-range disorder of the order parameter. We thus establish the separation between the nontrivial monopole thermodynamic behavior and criticality. Finally in Sec. V we discuss our results in the larger context of O(N) scalar theories in D dimensions. We argue that the criteria of Sec. II are sufficient to determine whether topological defects undergo an unbinding transition.

II. FREE ENERGY CONSIDERATIONS FOR O(N) POINT DEFECTS IN D DIMENSIONS

We can gain insight into the importance of topological excitations in O(N) models in D dimensions as vehicles of disorder by estimating the free energy associated with new pair excitations. Later we will specialize to two particular cases, those of vortices in 2D and of global monopoles in 3D, whose thermodynamics we investigate in detail in Sec. III. The line of argument used in this section follows the original reasoning by Kosterlitz and Thouless [18] in motivating the topological transition in the 2D XY model, with appropriate generalizations.

To be definite we consider a general O(N)-symmetric $\lambda\phi^4$ theory in D spatial dimensions. The Hamiltonian is written as

$$\mathcal{H}[\phi]=\int d^D\mathbf{x}\left\{\frac{1}{2}|\nabla\phi(\mathbf{x})|^2+\frac{\lambda}{4}[|\phi(\mathbf{x})|^2-\eta^2]^2\right\}, \quad (1)$$

where $\phi(\mathbf{x})$ is an N-component real field and $|\phi|^2=\phi(x)\phi^T(x)$.

The O(N) symmetry of Eq. (1) breaks spontaneously at low temperatures to O($N-1$), and the field acquires a nonzero expectation value. The degenerate set of minima lies on a S_{N-1} sphere. It follows that the homotopy group $\pi_{N-1}(S_{N-1})=Z$, the group of integers, which implies that topological solutions with integer charge exist in the spectrum of the theory. In $D=N$ dimensions these are point defects. The best know cases are the kink (or domain wall) in $D=N=1$, the global vortex for $D=N=2$, and the global monopole (or hedgehog) in $D=N=3$.

These topological defects are classical static solutions; i.e., they are (local) energy minima satisfying $\delta H/\delta\phi=0$. In D dimensions point defects are radially symmetric solutions. The integer topological charge of these configurations implies a singularity at their origin ($r=0$), which forces the field amplitude $\varphi(r\to 0)\to 0$. For large r it is energetically necessary that the field amplitude approach the minimum of the potential $\varphi(r\to 0)\to\varphi_0=\eta$.

These boundary conditions do not guarantee that the defect's energy is finite. In fact for $D\geqslant 2$ the energy of topo-

logical defects still diverges in the infinite-volume limit as a consequence of the phase gradient terms, which dominate the energy far from the singularity at $r=0$. These phase gradients lead to an asymptotic form of the energy, for large l,

$$E \simeq \int_{|\mathbf{x}|<l} d\mathbf{x} \frac{1}{2} |\nabla \phi|^2 \propto \varphi_0^2 n_q^2 \int_0^l dr r^{D-1} \frac{1}{r^2}, \tag{2}$$

where n_q is the topological charge of the field configuration.

The diverging energy of a single defect for $D \geqslant 2$ prohibits it from occurring as a fluctuation in thermal equilibrium in the infinite-volume limit. Instead, defects can occur in defect-antidefect multipoles (usually pairs), which due to mutual screening can then have finite energy, a continuous function of their separation. In the case of a pair, the charge separation introduces a natural cutoff to Eq. (2) which can be used as an estimate for the energy of a pair of size l. This naive expectation may be changed for $N=D>3$ [19], where the minimal energy configuration between two topological defects was argued to be one in which the far field is rotated to a uniform phase everywhere in space, apart from the region between the defects, where energy is concentrated and which behaves as a string [20]. Then the interaction potential between two point topological defects in $D=N>3$ will be of the same qualitative form as in $D=N=3$, although the associated string tension will differ quantitatively (it is expected to increase with N).

The simplest interesting example of interacting point defects is that of vortices in $D=2$. The vortex-antivortex dipole has a field

$$\begin{aligned} V_{D=2}^{\text{dipole}}(r) &\simeq -\varphi_0^2 n_q^2 [\ln(|\vec{r}+\vec{l}/2|) - \ln(|\vec{r}-\vec{l}/2|)] \\ &= -\varphi_0^2 n_q^2 \left[\frac{\vec{r}\cdot\vec{l}}{r^2} + O\left(\frac{l^2}{r^2}\right) \right], \end{aligned} \tag{3}$$

where $\vec{l}$ is the vector connecting the positive to the negative charge in the pair. As a consequence of Eq. (3) a point vortex far away from the dipole interacts with it via a potential inversely proportional to distance. Two well-separated pairs then interact with a potential

$$V_{D=2}^{\text{pairs}}(r) \simeq \varphi_0^4 n_q^4 \left[\frac{\vec{l}_1\cdot\vec{l}_2 - 2(\hat{r}\cdot\vec{l}_1)(\hat{r}\cdot\vec{l}_2)}{r^2} + O\left(\frac{l^3}{r^3}\right) \right], \tag{4}$$

where $\vec{l}_1$ and $\vec{l}_2$ are the separation vectors within each of the pairs, $\vec{r}$ is the vector connecting the center of the two pairs, and $\hat{r}=\vec{r}/r$. Thus a dilute gas of weakly interacting vortex pairs can exist at low temperatures.

Global monopoles have stronger linearly confining potentials. Their dipoles therefore behave as

$$\begin{aligned} V_{D=3}^{\text{dipole}}(r) &\simeq -\varphi_0^2 n_q^2 [|\vec{r}+\vec{l}/2| - |\vec{r}-\vec{l}/2|] \\ &= -\varphi_0^2 n_q^2 \left[\hat{r}\cdot\vec{l} + O\left(\frac{l^2}{r}\right) \right]. \end{aligned} \tag{5}$$

Although finite, the potential of this dipole is still substantial. Two well-separated pairs of monopoles then interact via

$$V_{D=3}^{\text{pairs}}(r) \simeq \varphi_0^4 n_q^4 \left[\frac{\vec{l}_1\cdot\vec{l}_2 - (\hat{r}\cdot\vec{l}_1)(\hat{r}\cdot\vec{l}_2)}{r} + O\left(\frac{l^3}{r^2}\right) \right]. \tag{6}$$

Since the interacting potential decreases inversely with separation, we see that monopole pairs can similarly exist in a dilute, weakly interacting state, but also that their mutual interactions are stronger than between vortex pairs. As we will see below this characteristic affects the thermodynamics of monopoles relative to vortices considerably. We remark in passing that the leading interaction between monopole pairs, apart from polarization inner products, behaves in 3D as the Coulomb potential. The Coulomb gas in 3D has a transition, associated with the familiar process of ionization, which is a smooth analytical crossover. In terms of monopole pairs this transition would occur between a phase of free pairs gas and another where monopole pairs become bound to form clusters. If it occurs, we may then expect that this monopole pair transition will not lead to critical (i.e., nonanalytic) behavior.

To estimate the free energy of a pair of defects we must finally estimate its entropy $S=\ln(\Omega)$, where Ω is the number of states of the pair. Ω is proportional to the surface of the $D-1$ sphere of radius l, i.e., the number of configurations a pair can take when rotated around its center of mass.

Then the single-pair free energy in arbitrary dimension D is

$$\begin{aligned} F_{D=2}(l) &\simeq E_c + a_D \varphi_0^2 \ln(l) - T b_D \ln(l), \\ F_{D>2}(l) &\simeq E_c + a_D \varphi_0^2 l^{D-2} - T(D-1) b_D \ln(l), \end{aligned} \tag{7}$$

where E_c accounts for the total core energy of the two defects in the pair and a_D and b_D are geometrical dimensionless constants dependent on the number of spatial dimensions.

We emphasize that in these considerations we neglected the effects of other defect pairs. Qualitatively these will reduce the free energy of the new pair relative to the above estimates, as they will tend to orient themselves in order to (partially) screen the new charges. Thus Eq. (7) should be thought of as an overestimate.

The free energy of the pair gives us a qualitative measure of its probability in equilibrium $P(l) \propto e^{-F(l)/T}$. We will explore this relationship further in Sec. III. For now we note that for $D=2$ both the energy and entropy terms behave logarithmically with l and the overall sign of the free energy for large pairs depends on the temperature, as noticed by Kosterlitz and Thouless [18]. In the low-T regime F grows with charge separation, leading to the suppression of large pairs. For high temperatures the entropy term is dominant and large pairs have negative free energy. This suggests the existence of a high-T phase characterized by the unbinding of defect-antidefect pairs and the production of free charges. This is the essential idea behind the Kosterlitz-Thouless mechanism for the O(2) 2D transition.

For higher dimensions $D>2$ the energy term dominates at large l for *all* temperatures and large pairs always remain

exponentially suppressed. This simple argument suggests that there is no unbinding topological transition for $D>2$ in global models and that defects remain tightly bound for all T. In order to destroy this picture it is necessary that the behavior of the bare energy and/or number of configurations with l would change due to interactions with other defect multipoles. Such behavior is not seen in the Kosterlitz-Thouless transition where the effect of other pairs softens the field modulus φ_0 (the superfluid density or spin wave rigidity), leading to a renormalized value of the transition temperature but not to a different kind of transition. In Eq. (7) we have taken the pair energy to be determined by a simple cutoff of the single-charge total energy (2). Our conclusions would remain unchanged if as suggested in [19] for $D>2$ the interaction becomes linear as the field's interacting core collapses into a string connecting the two charges in the pair. The entropy term would still be dominated by the interaction energy in the same way as for $D=3$.

Thus we have reached the conclusion that no unbinding topological transition should ever occur for $N=D>2$. We put this expectation to the test in Sec. III, where we study comparatively the thermodynamic behavior of both vortices in 2D and global monopoles in 3D.

We devote the remainder of this section to a few additional remarks about the applicability of the free energy considerations of defect pairs to more general circumstances. An interesting limit is that of systems that remain disordered due to topological configurations down to $T=0$. In the class of models of Eq. (1) only the case of the $N=1\lambda\phi^4$ theory (or the Ising model) in 1D has this property, due to the presence of kinks (or domain walls). In gauge+Higgs field theories the physical properties of topological solutions change radically because the phase gradients, which dominate the energetics of global defects, become pure gauge transformations and carry therefore no energy. This property is a direct result of the Higgs mechanism. The phase gradients correspond to Nambu-Goldstone modes, each associated with a generator for the remaining unbroken symmetries. In the Higgs mechanism these massless modes are ''eaten'' by the gauge field, which in turn acquires a mass. Thus the total energy of gauge defects is concentrated in their cores and falls off exponentially with distance. Then gauge topological charges interact via a short-range potential, in contrast to global defects. This interaction energy can typically be neglected or treated effectively, as a change of the core energy, in our thermodynamic estimates.

By repeating the free energy argument with core terms only we see that the entropy contribution is dominant for all temperatures, for large separations in $D\geqslant 2$. This implies that for large enough separation defect-antidefect pairs are always likely fluctuations and suffer no Boltzmann suppression down to $T=0^+$. This ''condensation'' of free topological excitations can explain striking properties of non-Abelian gauge theories [21]. The thermodynamic spectrum of these models should then be characterized by the existence of a dilute gas of free defects at low temperatures. The numerical verification of this expectation is presently the subject of intense research. Hints of this behavior have recently been found numerically; see, e.g., [22], for the case of a SU(2) lattice-gauge theory in 3D, which possesses 't Hooft–Polyakov magnetic monopoles—the direct analogs of the global monopoles in Eq. (1) for $N=D=3$.

III. CHARGE CLUSTERING AND THE KOSTERLITZ-THOULESS TRANSITION

As outlined in Sec. II the behavior of a system of charges with logarithmic interactions in 2D (the 2D Coulomb gas) is well known, underpinning the topological transition in the O(2) 2D model. In this section we develop diagnostics that allow us to measure, in numerical studies of the equilibrium partition function, the critical properties of topological point charges. Later we will use the Kosterlitz-Thouless behavior as the benchmark for a charge unbinding transition of $N=D=3$ monopoles.

Rather than using a discretized two-dimensional version of the Hamiltonian in Eq. (1) we chose to study the 2D XY model which belongs to the same universality class. This choice has the advantage that the XY model thermodynamics has been extensively studied, both analytically and via large-scale numerical simulations. Consequently its critical properties are well known quantitatively, including dimensionful quantities such as the Kosterlitz-Thouless transition temperature T_{KT} and the temperature at which the specific heat peaks T_{CV}.

The XY model consists of a set of two-dimensional unit-length spins with nearest-neighbor interaction. The Hamiltonian is given by

$$\mathcal{H}[\{\mathbf{s}\}]=-J\sum_{(ij)}\mathbf{s}_i\cdot\mathbf{s}_j, \tag{8}$$

where the sum is over all pairs of nearest-neighbor sites and we take $J=1$.

All quantities below were obtained via standard Monte Carlo generation of large ensembles on a lattice of size 128^2. For each temperature we obtained a set of 2000 independent configurations, from which we measured global properties of the vortex population. Local quantities not involving use of time-consuming cluster algorithms were averaged over larger ensembles. The vortex content of each field realization is determined by identifying integer spin windings around the lattice plaquettes. The values for the two characteristic temperatures, $T_{\mathrm{KT}}=0.89$ and $T_{\mathrm{CV}}=1.03$, were obtained from the literature (see, e.g., [23–25]) and are confirmed below. In particular we checked that the specific heat peaks at T_{CV} within statistical error.

Figure 1 shows the temperature-dependent density of vortex pairs $\rho_{\mathrm{vv}}(T)$ defined as the fraction of lattice plaquettes occupied by a positive charge. Note that although the total vortex density $\rho_{\mathrm{vv}}(T)$ increases with temperature it does not show a clear change of behavior at either T_{KT} or T_{CV}. This is not surprising since the system does not undergo a second-order phase transition, and the critical singularities are much weaker in nature. In particular the properties of a few large vortex pairs, crucial for the onset of phase disorder, are masked in $\rho_{\mathrm{vv}}(T)$ by the existence of many more small pairs.

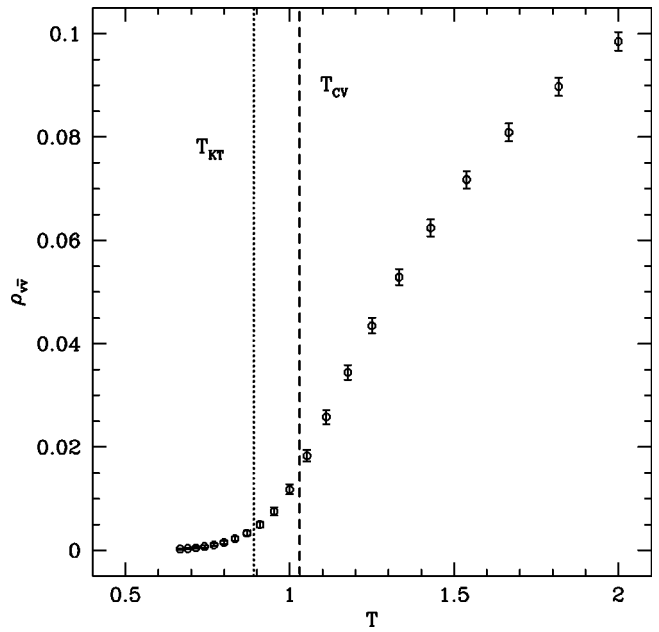

FIG. 1. The plaquette density of vortex pairs for the 2D *XY* model. Error bars denote standard deviation over 4000 independent field realizations. Both the Kosterlitz-Thouless temperature T_{KT} and T_{CV}, at which the specific heat peaks, are shown. No signs of critical behavior are apparent in the total vortex density.

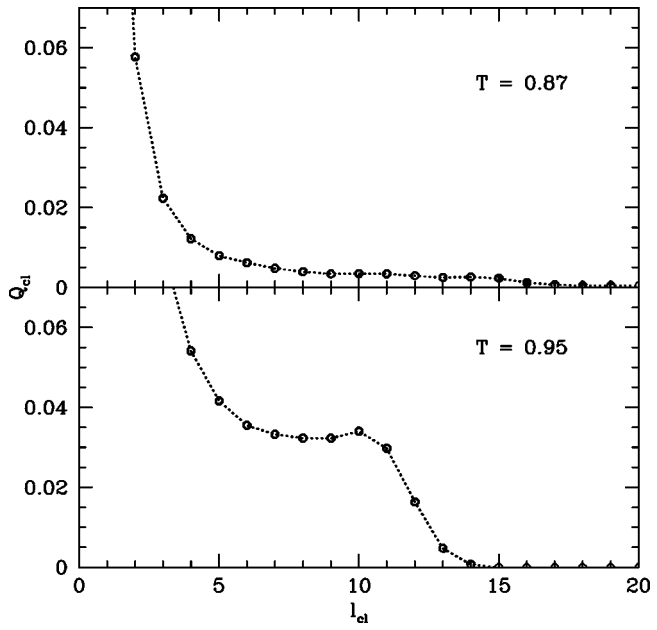

FIG. 2. Cluster charge Q_{cl} vs clustering length l_{cl} for a temperature slightly below (top plot) and above (bottom plot) the Kosterlitz-Thouless temperature, in the 2D *XY* model. Below the transition the mean charge decreases monotonically with l_{cl}. The clustering length l_{cl} for which $Q_{\mathrm{cl}}=0$ increases as $T\rightarrow T_{\mathrm{KT}}^{-}$. For $T>T_{\mathrm{KT}}$, Q_{cl} peaks at an intermediate value of l_{cl} before decaying to zero. Standard deviation error bars of order of the results not shown for clarity.

In order to see signs of the unbinding we must study the properties of the vortex population in greater detail.

To achieve this we must deal with the ambiguity involved in grouping vortices in pairs. To overcome this problem in the most general way possible we choose to group the vortices in each field realization into clusters, defined in terms of an adjustable length parameter l_{cl}. Vortices or antivortices—we do not distinguish between the two—separated by less than l_{cl} are collected in the same cluster. Thus, each cluster consists of the set of vortices and antivortices that lie within a distance l_{cl} of at least another element of the cluster.

The cluster decomposition is achieved efficiently by applying a generalization of the Hoshen-Kopelman algorithm [26], developed originally for studies of percolation. l_{cl} is successively increased, starting from the lattice spacing, the smallest length scale in the problem. For each l_{cl} we measure a set of cluster properties. In particular the topological charge properties of clusters are ideal diagnostics in the search for signs of a charge unbinding phase transition.

As a consequence of our choice of periodic boundary conditions the sum over the charge of all clusters in the volume is always zero. To quantify the typical charge of a cluster, we define, for each choice of l_{cl}, a mean cluster charge Q_{cl}. Here Q_{cl} results from adding up the absolute value of the charge Q of each cluster in a given realization and dividing the result by the total number of clusters, i.e.,

$$Q_{\mathrm{cl}}=\frac{1}{N_{\mathrm{clusters}}}\sum_{\mathrm{clusters}}|Q|. \tag{9}$$

Figure 2 shows $Q_{\mathrm{cl}}(l_{\mathrm{cl}})$ for two different values of the temperature around T_{KT}.

The behavior of Q_{cl} at low temperatures can be understood in terms of the properties of a dilute distribution of vortex-antivortex pairs. A vortex and an antivortex will be in the same cluster if their separation is smaller than the chosen l_{cl}. If the distance between different pairs is large, all pairs with separation smaller than l_{cl} will be in neutral clusters. In this case the charged clusters will consist only of single charges from pairs with separation larger than l_{cl}. With increasing clustering length, Q_{cl} should then decrease, reaching zero when l_{cl} becomes of the order of the largest pair in the sample. At this length all clusters become neutral. We then define L_{neutral} by $Q_{\mathrm{cl}}(L_{\mathrm{neutral}})=0$, a measure of the size of the largest pairs at a given temperature.

The top plot in Fig. 2 illustrates the typical behavior of Q_{cl} just below T_{KT}. $Q_{\mathrm{cl}}(l_{\mathrm{cl}})$ has a long tail for large values of the clustering length (up to $l_{\mathrm{cl}}\simeq 20$), signaling the presence of large pairs. For lower temperatures, Q_{cl} decays faster. In Fig. 3 we plot the variation of L_{neutral} with T. Up to the Kosterlitz-Thouless temperature L_{neutral} increases as pairs with larger and larger separations are produced.

According to the standard picture of the KT transition, above T_{KT} free charges appear in the system. Their presence affects $Q_{\mathrm{cl}}(l_{\mathrm{cl}})$ because a population of free vortices changes the charge of otherwise neutral clusters. Thus we can no longer expect $Q_{\mathrm{cl}}(l_{\mathrm{cl}})$ to decay monotonically. In fact we observe that above the transition Q_{cl} displays a peak at a finite value of the clustering length, which we define as L_{peak}. With increasing temperature the value of L_{peak} de-

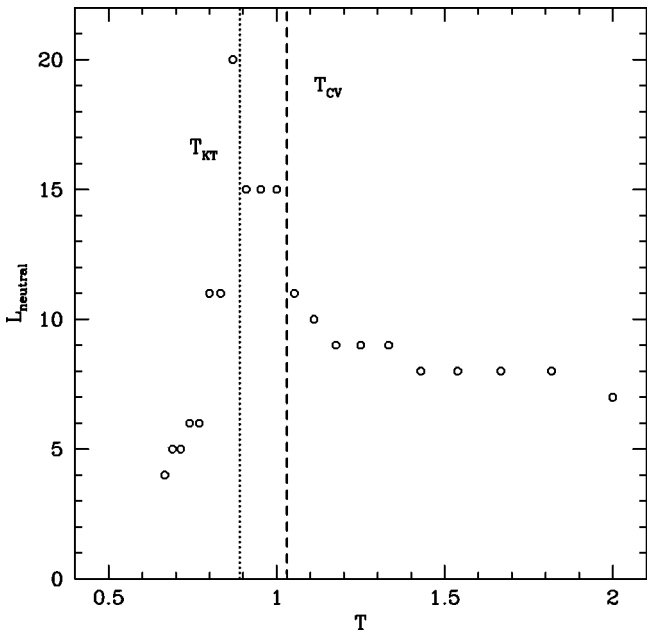

FIG. 3. The smallest clustering length L_{neutral} at which all vortex clusters are neutral, vs T, in the 2D XY model. For low densities L_{neutral} corresponds to the separation of the largest pair in the (finite) ensemble.

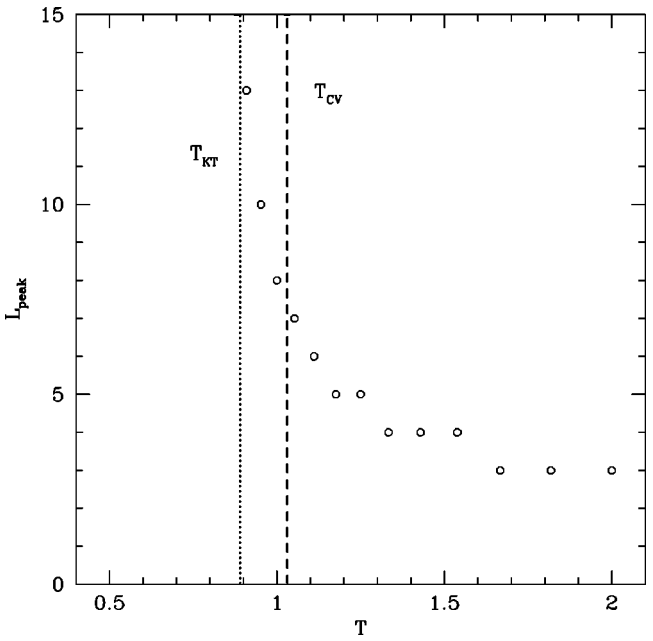

FIG. 4. Length for cluster charge peak in the 2D XY model. For $T>T_{\text{KT}}$, the length at which the cluster charge function peak decreases with T due to the production of higher densities of bound and unbound pairs. Below T_{KT} the mean charge decreases with l_{cl}; we define $L_{\text{peak}}=\infty$ in this case.

creases and the height of the peak increases. This is the result of a higher vortex density and, among them, more free charges. The increase in the density of free vortices also reduces the mean distance between them and moves the peak to lower l_{cl}. This behavior has the important characteristic that L_{peak} diverges as T_{KT} is approached from above. Higher free charge densities also lead to a decrease in L_{neutral} above T_{KT}.

The behavior of both L_{neutral} and L_{peak} is shown in Figs. 3 and 4, respectively. Both quantities show clear signs of critical behavior at T_{KT}, although the behavior of L_{neutral} is plagued by higher statistical uncertainty.

Note that pair unbinding is not the only way a set of point charges may display a change of properties. In general as temperature is increased two concurrent effects take place. The first is that pairs with larger separation and higher interaction energy are nucleated. The second is the production of more pairs at small separations. Depending on the interplay between these two trends a situation may be reached when the distance between different pairs is of the same order as the separation within each pair. In this case the system becomes dense (it percolates) and pairs become indistinguishable.

In order to determine the temperature at which pair percolation occurs in the 2D XY model we measured, for each configuration, the value of the clustering length at which all clusters become neutral $\langle l_{\text{max}}\rangle$ as well as the minimum l_{cl}, for which all vortices in the sample fall within the same cluster, L_{perc}. Note that $\langle l_{\text{max}}\rangle$ differs from L_{neutral} in the sense that $\langle l_{\text{max}}\rangle$ is a thermal average of the size of the largest pair in each sample, whereas L_{neutral} is the size of the largest pair in all samples in our ensemble. In this sense the peak in $\langle l_{\text{max}}\rangle$ reflects a maximal production of large pairs where the peak in L_{neutral} corresponds to the production a single very large (presumably infinite in the infinite-volume limit) pair.

For dense vortex systems, where there is no positive correlation between vortices and antivortices, $\langle l_{\text{max}}\rangle=L_{\text{perc}}$. This limit must be reached at high temperature as is indeed shown in Fig. 5. Moreover, we see that for $T<T_{\text{CV}}$ the length $\langle l_{\text{max}}\rangle<L_{\text{perc}}$. This includes the vicinity of T_{KT}, where pairs remain dilute enough that they can be identified. The density threshold where the vortex system becomes dense is $T\simeq T_{\text{CV}}$, but a precise identification would demand careful finite-volume scaling. In any case we also see that the approach to a dense state occurs seemingly continuously, without any clear signs of critical behavior. In this sense it may not be possible to associate it with a particular value of T.

We have now used cluster decomposition methods applied to the vortex population to characterize its critical properties. We found results in good agreement with previous, more limited, numerical studies [25] and with the theory. As the temperature is increased free vortices first appear at T_{KT} and are maximally produced approximately at T_{CV}, where the vortex system becomes dense and the concept of a vortex pair ceases to be meaningful.

IV. MONOPOLES IN THE 3D O(3) MODEL

A. Thermodynamics of the model

In this section we apply the tools developed in the context of the Kosterlitz-Thouless transition to a 3D scalar field theory with O(3) symmetry. Our analysis will be based on a discretized version of a $\lambda\phi^4$ theory, Eq. (1). We start by establishing its thermodynamic properties. In particular we

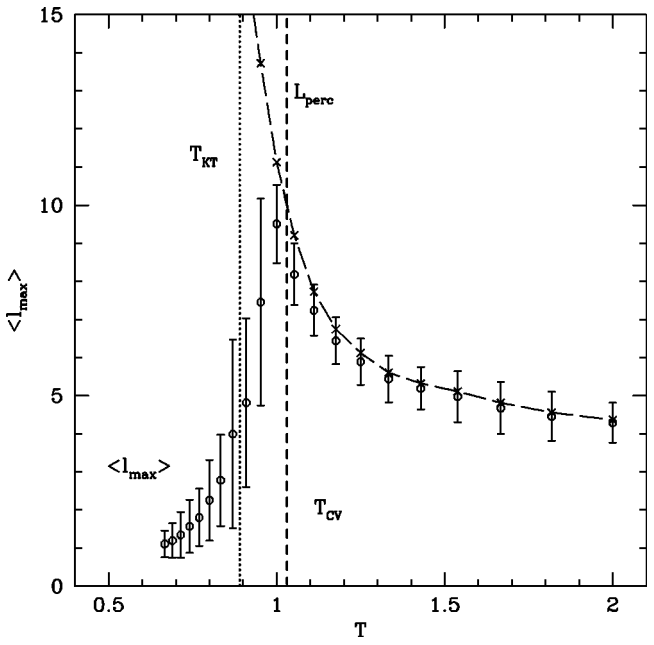

FIG. 5. Mean clustering length for neutral clusters $\langle l_{\max}\rangle$ in the 2D *XY* model, error bars corresponding to standard deviation over 2000 field samples. The dashed curve shows the clustering length for which all charges are gathered in a single cluster, standard deviation of the same order as for $\langle l_{\max}\rangle$, not shown for clarity. When the two curves meet near T_{CV} the system becomes dense.

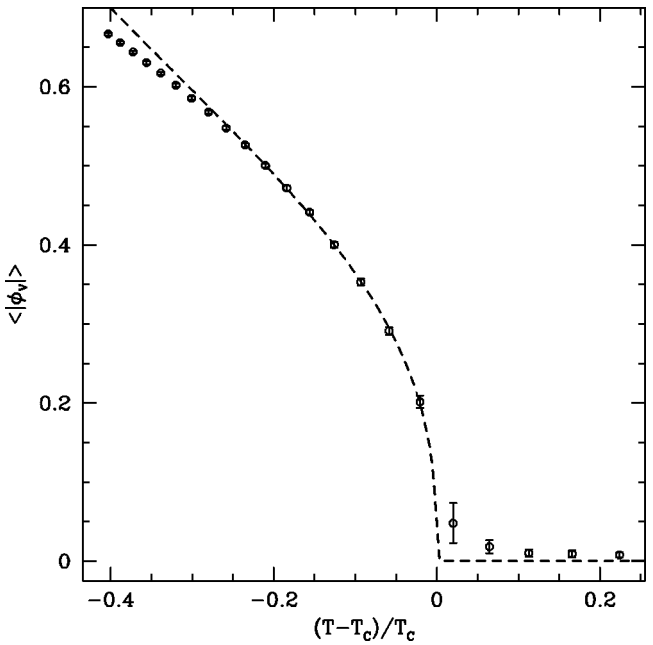

FIG. 6. Order parameter for the 3D O(3) model and corresponding power-law fit in the critical region. The temperature has been rescaled to $(T-T_c)/T_c$ setting $T_c=0.41$ as determined from the fit. Error bars denote standard deviation over an ensemble of 200 independent field realizations.

will be interested in determining the value of the critical temperature T_c at which the model displays a second-order phase transition.

In order to generate a Boltzmann distributed ensemble of field configurations we have evolved a second-order in time Langevin field equation (see [27] for more details). For our purposes this is equivalent to using a Monte Carlo or cluster algorithm. The advantage of the Langevin equation is that it can be easily generalized for time-dependent systems. In a future publication the equilibrium states generated in this way will be taken as initial conditions for real time out-of-equilibrium studies [28].

The procedure is as follows. We evolve the three-component real scalar field in time with the equation of motion

$$(\partial_t^2-\nabla^2)\phi_i-m^2\phi_i\sum_{j=1,3}\phi_j^2+\lambda\phi_i+\eta\dot{\phi}_i=\Gamma_i, \quad (10)$$

where $i\in\{1,2,3\}$. We discretize this scheme using a staggered-leapfrog method with time step $\delta t=0.04$. The random force $\Gamma_i(x,t)$ is a Gaussian distributed field with temperature T as determined by the fluctuation-dissipation theorem. Γ_i is characterized by

$$\langle\Gamma_i(x)\rangle=0, \quad \langle\Gamma_i(x)\Gamma_j(x')\rangle=\frac{2\eta}{T}\delta_{ij}\delta(x-x'). \quad (11)$$

The value of the dissipation coefficient η does not influence the equilibrium results and in our simulations we chose $\eta=1.0$ to ensure rapid convergence. The lattice spacing was set to $\delta x=0.5$ and the model parameters chosen to be $m^2=1.0,\lambda=1.0$. We used a computational domain with $L=100$ points per linear dimension. Both local and global observables were measured over at least 200 independent field realizations.

As an order parameter we have used the norm of the spatially averaged field $\langle|\phi_V|\rangle$, defined as

$$\langle|\phi_V|\rangle=\left\langle\sqrt{\sum_{i=1}^{3}\left(\frac{1}{V}\int_V d\mathbf{x}\phi_i(\mathbf{x})\right)^2}\right\rangle, \quad (12)$$

which is analogous to the magnetization in spin models.

Figure 6 shows the temperature dependence of $\langle|\phi_V|\rangle$. For $T>T_c$, $\langle|\phi_V|\rangle$ vanishes. Near but below T_c, the order parameter displays universal critical power-law behavior

$$\langle|\phi_V(T)|\rangle=B\left(\frac{T_c-T}{T_c}\right)^{\beta}, \quad \beta>0, \quad (13)$$

which is the analog of the magnetization density in spin models. Here β is the universal critical exponent associated with the behavior of the magnetization below T_c and is not to be confused with the inverse temperature elsewhere. By fitting the numerical values for $\langle|\phi_V|\rangle$ to Eq. (13) we are able to measure the critical temperature obtaining $T_c=0.41$. This sets a reference point, the most important scale in the system. We also compute the critical exponent $\beta=0.36$. This is in good agreement with both recent theoretical and large-scale Monte Carlo estimates for the critical exponent which give $\beta=0.366(2)$ and $\beta=0.3685(11)$, respectively (see, e.g.,

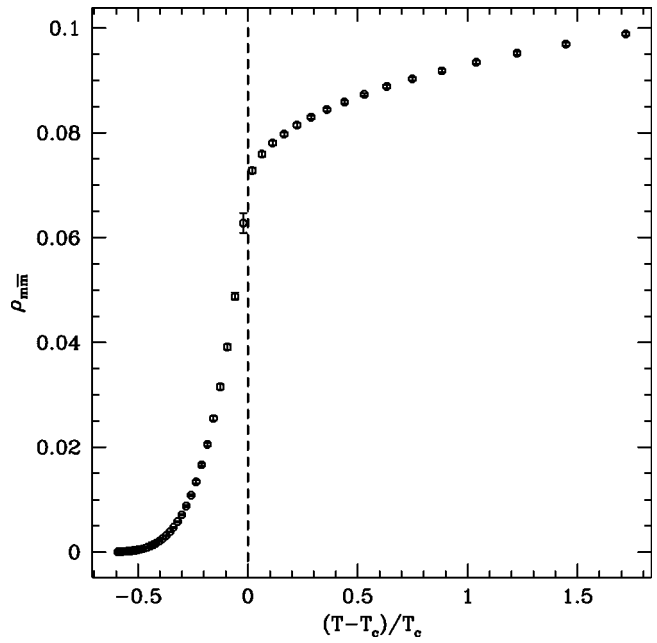

FIG. 7. The mean plaquette density of monopole pairs $\rho_{m\bar{m}}$ vs reduced temperature for the 3D O(3) model; error bars as in Fig. 6.

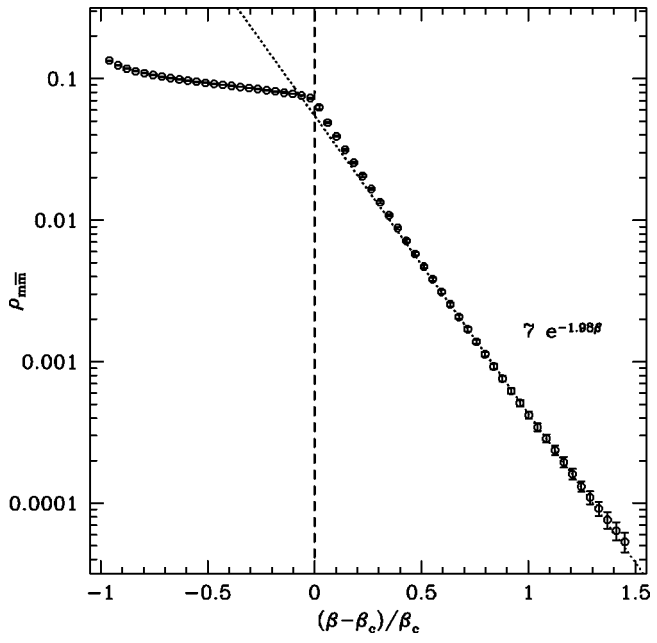

FIG. 8. Fit for the mean density of monopoles to $A\exp(-E_0/T)$; error bars as above. In the low-temperature regime we obtain $A=7.0\pm0.6$ and $E_0=1.98\pm0.02$, fitting the first 23 data points. Below T_c the density displays near exponential behavior down to $T=0$.

[29] and references therein) and provides a check on the accuracy of our numerical setup.

B. Monopole statistics

We are now ready to analyze the properties of the equilibrium global monopole population. For each field realization monopoles and antimonopoles are identified by measuring the three-dimensional winding number of the field around each cubic lattice cell. The algorithm used is based on a higher-dimensional generalization of the geodesic rule traditionally used for identifying strings in O(2) theories [30]. Details of this procedure are given in Appendix B.

Figure 7 shows the density of monopole-antimonopole pairs (defined as the total positive charge in the computational domain divided by the number of lattice sites) versus temperature. The total monopole density $\rho_{m\bar{m}}$ increases smoothly with T and its derivative peaks at the critical point, signaling the second-order phase transition. Above T_c the rate of increase diminishes and the total pair density converges slowly to approximately $\rho_{m\bar{m}}\rightarrow 0.17$ as $T\rightarrow\infty$ (not shown).

Figure 8 shows a log-linear version of Fig. 7 illustrating how over nearly the whole temperature range below T_c, $\rho_{m\bar{m}}$ is well fit by an exponential $\rho_{m\bar{m}}=Ae^{-E_0/T}$. Only very near the critical point does the fit fail to follow the density curve accurately. This behavior suggests that the increase in the total monopole density is dominated by the creation of large numbers of minimum-size pairs, each with typical energy $E_0\simeq 2.0$.

An understanding of this behavior can be obtained by evaluating the partition function for monopole pairs under certain simplifications. If we assume pairs are independent, i.e., if we neglect pair-pair interactions and volume exclusion effects, the partition function for a pair is

$$Z(T)=1+\sum_{\text{pairs}} e^{-E_p/T}, \tag{14}$$

where the sum is taken over all single-pair internal configurations; i.e., it excludes translational modes. We take the pair energy to be of the form

$$E_p=E_c+\sigma l, \tag{15}$$

where l is the monopole-antimonopole separation in units of lattice spacing. In the continuum the simplest way to compute $Z(T)$ would be to use the approximate expression for the free energy, Eq. (7). While this should be valid for large values of the pair size, such an evaluation of the number of states breaks down relative to that on the lattice, especially when l becomes of the order of the lattice spacing. Since we expect the monopole population to be dominated by small pairs, the continuum approximation would be a significant source of error. To circumvent this problem we calculate the partition function by evaluating numerically the sum in Eq. (14) over all possible lattice configurations of a pair with fixed center, for a given choice of E_c and σ. In this way the number of pair configurations on the lattice and, therefore, the entropy are calculated exactly.

Monopole thermodynamic averages can be easily evaluated from $Z(T)$. The total pair density per site is given by

$$\rho_{m\bar{m}}(T)=\frac{Z(T)-1}{Z(T)}. \tag{16}$$

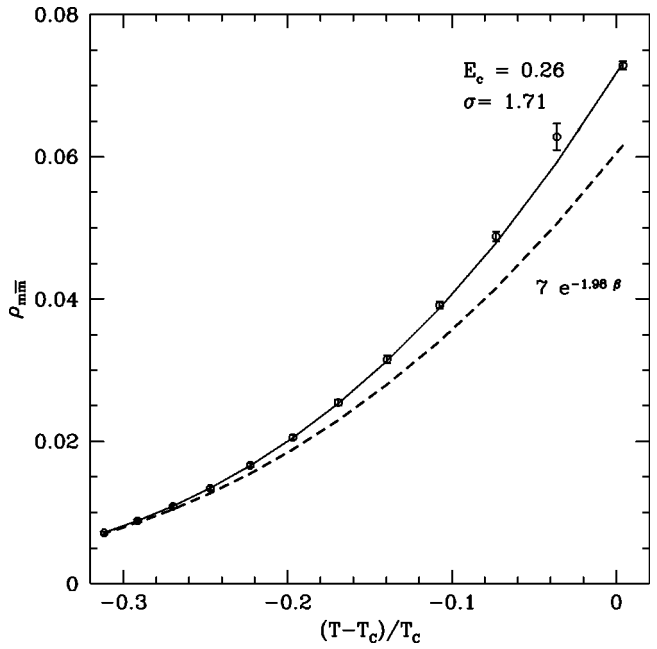

FIG. 9. Numerical data for the total pair density and corresponding fits near T_c; error bars as in Fig. 7. The energy varying theoretical curve (solid line) was fitted to the 18 lowest-temperature points (not shown in the plot) up to $(T-T_c)/T_c=-0.25$. The simple exponential fit (dashed line) fails to follow the numerical curve up to T_c, indicating relevant production of higher-energy, larger separation pairs in the critical region. The varying energy fit on the contrary matches the data well up to the critical point.

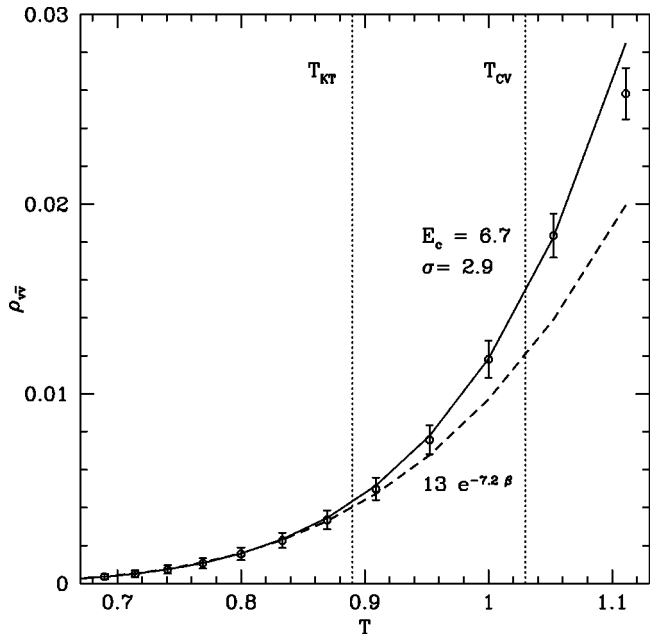

FIG. 10. Same as Fig. 9 for the 2D *XY* model. The theoretical curves were obtained by fitting the low-temperature data up to $T=0.75$, whereas the simple exponential (dashed line) fails to follow the observed density above T_{KT}. The curve obtained from the partition function, which includes pairs with all separations, matches the data well up to T_{CV}.

By allowing E_c and σ to take arbitrary values, we fit the predicted pair density to the numerical data. A χ squared fit leads to estimated values of the interaction parameters of $E_c \simeq 0.26$ and $\sigma \simeq 1.71$.

In Fig. 9 we compare the monopole density $\rho_{m\bar{m}}$ obtained in this way to the numerical data and to the simple exponential fit discussed before. Clearly taking into account pairs with variable separation improves the estimate leading to precise results up to T_c. It remains true, however, that the monopole thermodynamics is always dominated by very small pairs. Using the fit results for E_c and σ we obtain the following energies for the smallest pairs allowed on the lattice: $E(1)=1.97$,$E(\sqrt{2})=2.68$, and $E(\sqrt{3})=3.22$. Considering the contribution of the first three terms in the partition function already leads to a very reasonable approximation to $Z(T)$:

$$Z(T)=1+6e^{-1.97/T}+12e^{-2.68/T}+8e^{-3.22/T}. \qquad (17)$$

This gives $\rho_{m\bar{m}}(T_c)=0.07$, in good agreement with the measured value (the integer pre-factors are the number of different lattice configurations for a pair at these separations).

The value measured for σ is considerably lower than the one obtained from the single-monopole classical estimate in Sec. II. Evaluating Eq. (2) exactly we have for the single-pair energy $E_p=E_c+4\pi m^2/\lambda\times l$, which leads to $\sigma=2\pi$ in lattice spacing units ($\delta x=0.5$). The difference between this classical value of σ and its value inferred from fitting the thermodynamic monopole density is a consequence of strong medium-dressing effects, resulting both from the influence of other monopole pairs and from interactions with the spin-wave degrees of freedom.

In any case the unequivocal exponential behavior of the total density below the critical point implies that $\sigma \leqslant 2$. The quality of the fit using $\sigma=1.7$ and its success in predicting other features of the data (see below) suggest that one should not place exaggerated confidence in the classical single-monopole result.

In a previous publication [31] two of us predicted the value of the defect density at criticality for O(N) theories. This calculation assumes that fluctuations at T_c are Gaussian, with their scale-invariant connected two-point function characterized by the universal critical exponent η, the anomalous dimension. Using the value of $\rho_{m\bar{m}}=0.17$ at infinite temperature as a normalization (see [31] for details) leads to a predicted $\rho_{m\bar{m}}(T_c)\simeq 0.07$ for O(3) in 3D, in good agreement with the present numerical measurements.

A similar calculation of the temperature dependence of the vortex pair density can be done for the 2D *XY* model. As in the monopole case, the low-temperature Monte Carlo data is reasonably well fitted by an exponential. Assuming a pair energy of the form $E_p=E_c+\sigma\ln(l)$ and calculating the partition function as before, the prediction can be improved leading to good results up to T_{CV} (see Fig. 10). The single-exponential fit for low T gives $E_0\simeq 7.2$ which compares well with a previous result of 7.5, measured by Gupta and Baillie [23]. The difference is probably due to our fit being based on low-T data points only. In the same article [23] Gupta and Baillie also obtained a different exponential fit in the temperature region between T_{KT} and T_{CV} with a higher value for

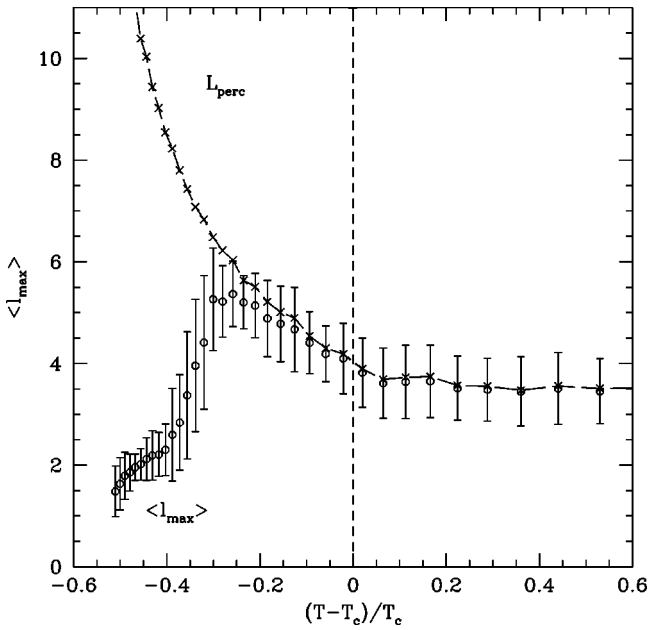

FIG. 11. Mean clustering length for neutral clusters (error bars correspond to standard deviation over 200 field samples) and percolation length (dashed curve, standard deviation error bars of the same order as for $\langle l_{\max}\rangle$, not shown for clarity) for the 3D O(3) model. The system becomes dense well below the critical temperature when the two quantities become comparable.

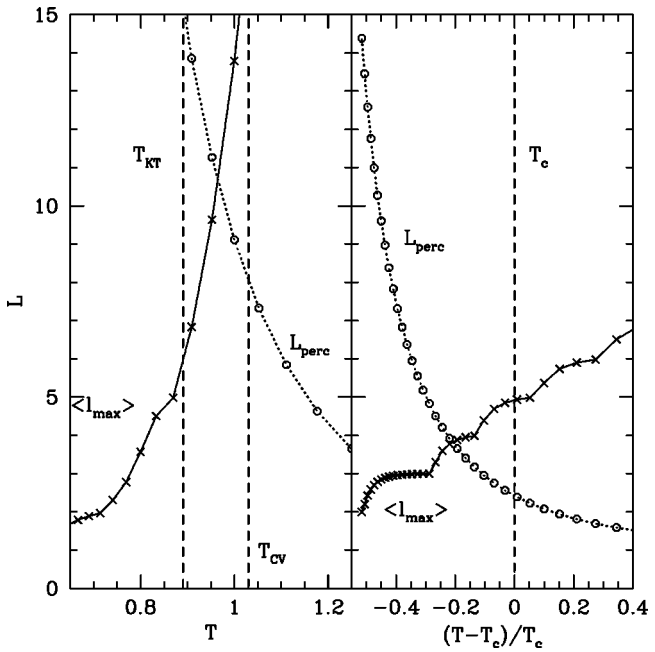

FIG. 12. Theoretical prediction for the temperature-dependent mean maximal pair size $\langle l_{\max}\rangle$ and pair separation $L_{\rm perc}$, for the 2D XY model (left) and the 3D O(3) model (right). At the temperature where the two curves cross, the system becomes dense and it is no longer possible to distinguish individual pairs. The steplike appearance of $\langle l_{\max}\rangle$ in the right plot is due to lattice discretization effects on l, which are apparent due to the small size of the monopole-antimonopole pairs.

E_0. Using the form (15) we are able to fit both temperature regimes obtaining the χ squared results $E_0 \simeq 6.7$ and $\sigma \simeq 2.9$.

Following in the footsteps of the 2D charge cluster analysis we now turn to the properties of monopoles in the O(3) 3D theory. Figure 11 shows $\langle l_{\max}\rangle$ and $L_{\rm perc}$ in terms of the reduced temperature in the critical region. The monopole ensemble becomes dense when the two length scales are comparable, $\langle l_{\max}\rangle \simeq L_{\rm perc}$, and it is no longer possible to identify isolated pairs. This happens at $(T-T_c)/T_c \simeq -0.25$, the temperature at which $\langle l_{\max}\rangle$ peaks, well below T_c. This behavior stands in striking contrast to that of vortices in the 2D case (see Fig. 5), where the vortex gas percolated only in the exponentially disordered phase at $T=T_{\rm CV}>T_{\rm KT}$.

It is important to realize that this behavior of monopoles is not in contradiction with maintaining long-range order up to T_c. The system of monopole-antimonopole pairs can become dense without disordering the field over large distances. This can be understood by considering a domain with radius much larger than the maximal pair size and is essentially the earlier result of Bitar and Manousakis [17]. Since the total field winding in the domain's surface is given by the total charge in its interior, its value will be zero. That is, finite pairs will not affect the long-range behavior of the field on scales larger than their size; only unbound charges can lead to the breakdown of long range order.

The proliferation of small pairs in the three-dimensional case is made possible by the fact that the core energy of the monopole is small when compared with the interaction potential. This leads to production of large densities of small pairs, while large pairs remain strongly suppressed by the fast growing linear interaction term. As a consequence the system percolates mostly due to a high-density population of small pairs at a temperature where large pair configurations have an exponentially negligible contribution to the thermodynamics.

To investigate this behavior we can use our approximate partition function to calculate $N(l)$, the density of pairs of size l, as

$$N(l)=Z^{-1}(T)n(l)e^{-E_p(l)/T}, \tag{18}$$

where $n(l)$ is the total number of configurations for a pair of size l. This expression can be readily evaluated numerically. We then use $N(l)$ to estimate the size of the largest pair in a computational domain by finding the value for l such that $N(l)\times L^D \simeq 1.0$, where L is the linear size of the computational volume. That is, we demand that in each computational volume there should be on average one pair of maximal size. This length scale corresponds to $\langle l_{\max}\rangle$. The value of $\langle l_{\max}\rangle$ estimated in this way is plotted against temperature for both models in Fig. 12.

In order to calculate the percolation temperature in this approximation we must estimate $L_{\rm perc}$. This can be done by assuming that the typical distance between pairs is of order of $1/\rho^{(1/D)}$, where ρ denotes either $\rho_{v\bar{v}}$ or $\rho_{m\bar{m}}$ depending on the dimension. This implies that we will have percolation when $\langle l_{\max}\rangle \simeq 1/\rho^{(1/D)}$. Figure 12 shows the temperature dependence of $L_{\rm perc}$, estimated as $1/\rho^{(1/D)}$, using the parameters from the previous density fits. The point where the two

curves meet defines the percolation temperature where the charge ensemble becomes dense. The values obtained agree reasonably well with the data. For the 3D O(3) case we find the percolation temperature to be $(T-T_c)/T_c \simeq -0.2$ with pairs of maximal size 4, compared to $(T-T_c)/T_c \simeq -0.25$, with the largest length of around 5.5 from the numerical results. For the *XY* model we obtain $T \simeq 0.96$, slightly below T_{CV}, but still clearly in the exponentially disordered phase and $l \simeq 10$, which coincides with the numerical result for the mean size of the largest pair per box at the percolation temperature.

V. CONCLUSIONS

We started this paper by using single-defect-pair free energetic arguments to predict that no pair unbinding transition should occur for point defects in O(N) models with global symmetries for $N=D>2$. We then verified this prediction by comparatively studying the defect thermodynamics of vortices and global monopoles occurring in typical configurations drawn numerically from canonical ensembles of the O(2) model in 2D and an O(3) field theory in 3D.

We measured in great detail the behavior of vortices across the Kosterlitz-Thouless transition and found it in agreement with the expectations of the theory, which predicts the appearance of free vortices at T_{KT}. In the O(3) model in 3D isolated single monopoles never occur. Instead the monopole ensemble transits from a dilute pair phase at low temperatures, to a dense monopole gas, through the nucleation of large numbers of tightly bound pairs below T_c. We have seen that this behavior is consistent with qualitative expectations based on the single-monopole pair energetics, which is characterized by a light core and a linearly confining interaction potential. Our quantitative treatment shows, however, that the bare parameters in the monopole potential—the monopole core energy E_c and string tension σ—are significantly renormalized by thermal medium effects.

The thermodynamic behavior of global monopoles is consistent with both a (noncritical) topological-charge conductor-to-insulator transition and the absence of long-range phase disorder at temperatures below T_c. Global monopoles in 3D do not behave like Coulomb charges, but rather more like static quarks, since they interact via a linearly confining potential. The conductor phase in this case cannot be reached by the nucleation of truly free isolated charges, as in the Kosterlitz-Thouless transition. It instead results from the fact that in a dense monopole gas charges can move freely by hopping from a nearby anticharge to another. Because local charge neutrality persists to all finite temperatures [17], the dense monopole gas does not lead to long-range disorder of the field phases (spins). Long-range phase fluctuations must therefore arise from different degrees of freedom, the spin waves. This is indeed the renormalization group picture of the transition, which correctly predicts all universal critical behavior. From this perspective we conclude that monopole excitations, although contributing to short-range disorder in the O(3) model in 3D, are incapable by themselves, because of their enslaving energetics, of producing long-range disorder at any finite temperature. This is not to say that their disordering influence can be completely neglected. Their effects must generate a short-distance nontrivial quantitative contribution to critical exponents, thus making the universality class in their absence different [14].

In this way we must conclude that there is a nontrivial interplay between monopoles and spin waves in the O(3) model and that the detailed nature of the critical behavior is changed if either are suppressed.

The generalization of these qualitative results to arbitrary $N=D>3$ is immediate. The potential between defects becomes steeper and steeper as a function of l, and topological excitations, just like monopoles in 3D, will never unbind. In this way topological excitations do indeed become more and more irrelevant, as N increases, for the physics of large length scales that characterizes thermodynamics in the critical domain of O(N) models.

We also see from this perspective that upon cooling the system most topological fluctuations will annihilate with a nearby antidefect, leading to small and quickly disappearing populations of topological defects. From this perspective global topological monopoles formed at a cosmological phase transition present no real danger of creating a ''monopole problem.''

We conclude by invoking a complementary view of the phase transition in O(N) models. There is clear evidence (and mathematical proofs in certain particular cases) that criticality in O(N) scalar models is equivalent to the percolation of so-called Wolff spin clusters [32]. Wolff clusters are built by forming bonds among adjacent spins according to a temperature dependent probability. Because of this probabilistic assignment, Wolff clusters are subsets of the set of clusters formed by associating all adjacent spins with the same orientation. Clusters formed by considering spins with the same orientation, without this probabilistic restriction, percolate below T_c. It is the typical size of these latter ''conventional'' clusters that is associated with defect densities, according to the Kibble-Zurek [10,11] theory of defect formation. Our observation of monopole percolation below T_c is compatible with this scenario. The interesting questions testing this hypothesis and determining the detailed relationship between Wolff clusters and topological excitations at criticality will be left for future work.

ACKNOWLEDGMENTS

This work is supported in part by the U.S. Department of Energy under cooperative research agreement No. DF-FC02-94ER40818. N.D.A. was supported by PPARC. M.K. acknowledges support from the Swiss National Science Foundation under Contract No. 83EU-062445. We would like to thank R. Durrer for helpful discussions. N.D.A. would like to thank G. Volovik and A. Schakel for useful suggestions.

APPENDIX A: ENERGETICS OF LINE DEFECTS IN *D* DIMENSIONS

The free energy arguments of Sec. II can be generalized to extended topological defects. In this appendix we consider the case of line defects.

Let us look first at the case of one-dimensional defects $N=D-1$. For a stringlike object the core energy is proportional to its length l, and the entropy can easily be calculated assuming that it behaves like a random walk. The number of different configurations for a closed random walk in a cubic D-dimensional lattice is given by

$$\Omega=(2D)^{l}(4\pi l)^{-D/2}\times l^{-1}. \tag{A1}$$

The first two terms count the number of possible closed random walk loops with l steps and the final factor takes into account the arbitrariness in the choice of initial point in the loop. We see that the entropy $S=\ln(\Omega)$ grows linearly with l. The free energy is then (omitting dimensionless constants)

$$F(l)\simeq\sigma l+E_I+T\left(\frac{D}{2}+1\right)\ln(l)-\ln(2D)Tl, \tag{A2}$$

where σ is the string tension and $E_I(l)$ the interaction energy for the loop. In general E_I is a function not only of the string length but also of its detailed shape. We start by considering the case when the interaction energy can be neglected. Then we see immediately that the system will undergo a phase transition above a certain T, characterized by the proliferation of long strings. This is because both the entropy and core energy have the same dependence on l, as was the case in the Kosterlitz-Thouless transition.

This set of approximations gives a reasonable description of the $D=2$ Ising model, where there is no long-range interaction between strings and probably also of strings in gauge theories in any dimension. In contrast to the case of monopoles, where the pair interaction was responsible for the confining phase at low T, here it is the core energy of the string that keeps it at a finite length.

The interaction energy is hard to estimate and depends in general on details of the underlying model as well as of particular configurations. We can make a rough estimate by assuming that the string remains a random walk and consequently that the distance between two points on the string is of order of $l^{1/2}$. Then if two distant string segments interact as pointlike defects in an $O(N-1),D-1$ theory, the loop energy will be given by

$$E_I(l)\simeq l\times l^{(D-3)/2},\quad D>3,$$

$$E_I(l)\simeq l\ln(l),\quad D=3. \tag{A3}$$

Clearly for $D>3$ the interaction term dominates over the entropy for all T, indicating the absence of a proliferating phase. The marginal case, for $D=3$, is harder to judge in this approximation, since the correction to the linear interaction is only logarithmic. In reality we have good evidence [33] that for 3D O(2) the string tension goes to zero at T_c and there is a percolation transition in the network, very close to the critical point, at which long strings spanning the volume appear.

For higher-dimensional defects the calculation of the entropy becomes much harder. For example surfaces can be topologically complicated, exhibiting holes and handles. The general trend seems to suggest that for fixed spatial dimension, the entropy of a typical defect configuration decreases with N. Since the interaction energy increases with the number of field components, we expect that for any D and above a certain N the free energy will always be dominated by the interaction component and proliferation of defects is prohibited at all finite temperatures. For $D=3$, for example, strings proliferate in the high-T phase for $N=2$ but no unbinding of charge pairs occurs for $N=3$.

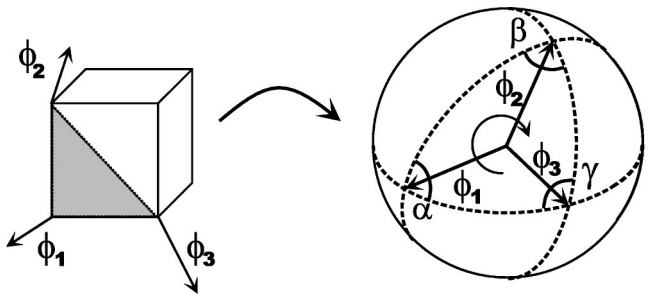

FIG. 13. The monopole charge in a cubic cell is identified by projecting the field vectors at every corner onto a unit sphere. Each triangle on the square faces cube is thus mapped onto a spherical triangle (the one with the smallest surface is chosen). The sum of the surface of all these triangles, divided by 4π, is then taken as defining the monopole charge inside the cubic cell.

APPENDIX B: DEFINING WINDING CHARGE ON THE LATTICE FOR GLOBAL THEORIES

We identify O(3) monopoles in a 3D cubic lattice by generalizing the well-known ''geodesic rule'' used in most cosmic-string lattice-based simulations [30].

We count the winding of the field vectors around each unit cell in our grid by using a ''smallest-area'' assumption. To this end, we triangulate the faces of each lattice cube and then map the O(3) field vector at all corners onto the unit sphere (the presence of a monopole depends only on the orientation of the field, not on its norm). For each triangular element in the cube's surface this defines a solid angle on the unit sphere (see Fig. 13). The sign of the solid angle is taken according to the handedness of the corners. Its value Θ can be calculated thanks to a formula that relates the area of the spherical triangle, defined by three vectors on a unit sphere, to the angles between the geodesic sides of the triangle:

$$|\Theta|=\alpha+\beta+\gamma-\pi. \tag{B1}$$

Summing the solid angles corresponding to all the 12 triangles in the cube's surface, we obtain $\Sigma\Theta=4\pi n$ where n is an integer taken to be the charge of the monopole inside the lattice cube. $|n|$ has an upper bound of 5 but in practice we rarely observe charges larger than 2 (which we interpret as two coincident unit charges).

[1] See, e. g., M. Tinkham, *Introduction to Superconductivity*, 2nd ed. (McGraw-Hill, New York, 1995).
[2] See, e.g., A.M. Polyakov, *Gauge Fields And Strings* (Harwood Academic, Chur, Switzerland, 1987).
[3] D.R. Nelson, in *Phase Transitions and Critical Phenomena*, edited by C. Domb and J. J. Lebowitz (Academic Press, New York, 1983).
[4] L.D. Landau, E.M. Lifshitz, and P. Pitaevskii, *Statistical Physics* (Pergamon Press, New York, 1980).
[5] N.D. Mermin and H. Wagner, Phys. Rev. Lett. **22**, 1133 (1966).
[6] A.J. Bray, Adv. Phys. **43**, 357 (1994).
[7] G.F. Mazenko, Phys. Rev. Lett. **63**, 1605 (1989).
[8] H. Kleinert, *Gauge Fields in Condensed Matter Physics* (World Scientific, Singapore, 1989).
[9] P.M. Chaitkin and T.C. Lubensky, *Principles of Condensed Matter Physics* (Cambridge University Press, Cambridge, England, 1995).
[10] T.W.B. Kibble, J. Phys. A **9**, 1387 (1976).
[11] W.H. Zurek, Nature (London) **317**, 505 (1985); Acta Phys. Pol. B **24**, 1301 (1993).
[12] See, e.g., A. Vilenkin and E.P.S. Shellard, *Cosmic Strings and Other Topological Defects* (Cambridge University Press, Cambridge, England, 1994).
[13] M.H. Lau and C. Dasgupta, Phys. Rev. B **39**, 7212 (1989).
[14] M. Kamal and G. Murthy, Phys. Rev. Lett. **71**, 1911 (1993).
[15] K. Huang, Y. Koike, and J. Polonyi, Int. J. Mod. Phys. A **6**, 1267 (1991).
[16] C. Holm and W. Janke, J. Phys. A **27**, 2553 (1994).
[17] K. Bitar and E. Manousakis, Phys. Rev. B **43**, 2615 (1991).
[18] J.M. Kosterlitz and D.J. Thouless, J. Phys. C **6**, 118 (1973); J.M. Kosterlitz, *ibid.* **7**, 1046 (1974).
[19] S. Ostlund, Phys. Rev. B **24**, 485 (1981).
[20] A. Achucarro and J. Urrestilla, Phys. Rev. Lett. **85**, 3091 (2000).
[21] A.M. Polyakov, Nucl. Phys. B **120**, 429 (1977).
[22] A.C. Davis, A. Hart, T.W.B. Kibble, and A. Rajantie, e-print hep-lat/0110154.
[23] R. Gupta and C.F. Baillie, Phys. Rev. B **45**, 2883 (1992).
[24] P. Olsson, Phys. Rev. B **52**, 4511 (1995); **52**, 4526 (1995).
[25] J. Tobochnik and G.V. Chester, Phys. Rev. B **20**, 3761 (1979); C. Bowen, D.L. Hunter, and N. Jan, J. Stat. Phys. **69**, 1097 (1992).
[26] J. Hoshen and R. Kopelman, Phys. Rev. B **14**, 3438 (1976).
[27] N.D. Antunes, L.M.A. Bettencourt, and W.H. Zurek, Phys. Rev. Lett. **82**, 2824 (1999), and references therein.
[28] N.D. Antunes, L.M.A. Bettencourt, and M. Kunz (unpublished).
[29] A. Pelissetto and E. Vicari, e-print cond-mat/0012164.
[30] T. Vachaspati and A. Vilenkin, Phys. Rev. D **30**, 2036 (1984).
[31] N.D. Antunes, L.M.A. Bettencourt, and A. Yates, Phys. Rev. D **64**, 065020 (2001).
[32] U. Wolff, Phys. Rev. Lett. **62**, 361 (1989); Nucl. Phys. B **322**, 759 (1989); see also P. Blanchard, S. Digal, S. Fortunato, D. Gandolfo, T. Mendes, and H. Satz, J. Phys. A **33**, 8603 (2000).
[33] N.D. Antunes, L.M.A. Bettencourt, and M. Hindmarsh, Phys. Rev. Lett. **80**, 908 (1998); N.D. Antunes and L.M.A. Bettencourt, *ibid.* **81**, 3083 (1998); K. Kajantie *et al.*, Phys. Lett. B **482**, 114 (2000); A.K. Nguyen and A. Sudbo, Phys. Rev. B **60**, 15 307 (1999).